



How accurate is the strongly orthogonal geminal theory in predicting excitation energies? Comparison of the extended random phase approximation and the linear response theory approaches

Katarzyna Pernal, Koushik Chatterjee, and Piotr H. Kowalski

Citation: *The Journal of Chemical Physics* **140**, 014101 (2014); doi: 10.1063/1.4855275

View online: <http://dx.doi.org/10.1063/1.4855275>

View Table of Contents: <http://scitation.aip.org/content/aip/journal/jcp/140/1?ver=pdfcov>

Published by the [AIP Publishing](http://aip.org)

Articles you may be interested in

Erratum: "How accurate is the strongly orthogonal geminal theory in predicting excitation energies? Comparison of the extended random phase approximation and the linear response theory approaches" [*J. Chem. Phys.* **140**, 014101 (2014)]

J. Chem. Phys. **140**, 189901 (2014); 10.1063/1.4876720

Excitation energies with linear response density matrix functional theory along the dissociation coordinate of an electron-pair bond in N-electron systems

J. Chem. Phys. **140**, 024101 (2014); 10.1063/1.4852195

Theoretical and numerical assessments of spin-flip time-dependent density functional theory

J. Chem. Phys. **136**, 024107 (2012); 10.1063/1.3676736

An accurate first principles study of the geometric and electronic structure of B_2 , B_2^- , B_3 , B_3^- , and B_3H : Ground and excited states

J. Chem. Phys. **132**, 164307 (2010); 10.1063/1.3389133

Electron correlation in the $3\Sigma_g^+ + 1$ and $2\Sigma_u^+ + 1$ excited state lithium molecule

J. Chem. Phys. **125**, 234102 (2006); 10.1063/1.2404665



NEW Special Topic Sections

NOW ONLINE
Lithium Niobate Properties and Applications:
Reviews of Emerging Trends

AIP Applied Physics Reviews

How accurate is the strongly orthogonal geminal theory in predicting excitation energies? Comparison of the extended random phase approximation and the linear response theory approaches

Katarzyna Pernal,^{1,a)} Koushik Chatterjee,² and Piotr H. Kowalski²

¹*Institute of Physics, Technical University of Lodz, ul. Wolczanska 219, 90-924 Lodz, Poland*

²*Faculty of Chemistry, Technical University of Lodz, ul. Zeromskiego 116, 90-924 Lodz, Poland*

(Received 5 October 2013; accepted 10 December 2013; published online 2 January 2014)

Performance of the antisymmetrized product of strongly orthogonal geminal (APSG) ansatz in describing ground states of molecules has been extensively explored in the recent years. Not much is known, however, about possibilities of obtaining excitation energies from methods that would rely on the APSG ansatz. In the paper we investigate the recently proposed extended random phase approximations, ERPA and ERPA2, that employ APSG reduced density matrices. We also propose a time-dependent linear response APSG method (TD-APSG). Its relation to the recently proposed phase including natural orbital theory is elucidated. The methods are applied to Li₂, BH, H₂O, and CH₂O molecules at equilibrium geometries and in the dissociating limits. It is shown that ERPA2 and TD-APSG perform better in describing double excitations than ERPA due to inclusion of the so-called diagonal double elements. Analysis of the potential energy curves of Li₂, BH, and H₂O reveals that ERPA2 and TD-APSG describe correctly excitation energies of dissociating molecules if orbitals involved in breaking bonds are involved. For single excitations of molecules at equilibrium geometries the accuracy of the APSG-based methods approaches that of the time-dependent Hartree-Fock method with the increase of the system size. A possibility of improving the accuracy of the TD-APSG method for single excitations by splitting the electron-electron interaction operator into the long- and short-range terms and employing density functionals to treat the latter is presented.

© 2014 AIP Publishing LLC. [<http://dx.doi.org/10.1063/1.4855275>]

I. INTRODUCTION

Geminal theories have emerged as a promising tool for including electron correlation energy in molecules.¹ They are based on the ansatz of antisymmetrized product of two-electron functions called geminals. The resulting optimization problem is, in general, involved unless geminals are restricted to be strongly orthogonal that leads to the antisymmetrized product of strongly orthogonal geminal (APSG) theory.^{2,3} The cost of optimizing the APSG energy is comparable to mean-field methods and recently an efficient optimization algorithm has been proposed.⁴ It is known that although the amount of dynamical correlation energy recovered by the APSG ansatz decreases with the system size the method is capable of capturing static correlation effects.^{1,5} In particular, it performs correctly when one bond is dissociated in a molecule.

APSG wavefunction is of a multireference nature, consisting of many determinants with high excitations. Therefore, APSG-based methods hold a promise of reproducing not only single but also double excitations at low computational cost. Another incentive for investigating the APSG methods lies in the fact that the APSG energy functional is of the form of the phase including natural orbital functional (PINO) introduced in Refs. 6 and 7. Understanding the limits of the

geminal theory may give hints on how to develop a PINO functional that could be useful for predicting excitation energies. In the past there were some attempts undertaken to employ the APSG wavefunction either within the Tamm-Dankoff approximation⁸ or in the coupled perturbed framework⁹ but no numerical results were presented. Only recently, first examples of excitation energies obtained by employing APSG density matrices in the extended random phase approximation equations (ERPA and ERPA2) have been presented.¹⁰ The proposed ERPA2 approach has been shown to be exact for singlet excitation energies of two-electron systems and to provide very accurate single and double excitations of beryllium atom and LiH molecule.

The goal of the paper is to present and discuss methods for computing excitation energies that employ the APSG ansatz, to investigate their performance for small molecules, and to make predictions for larger systems. We begin by introducing the APSG functional and showing its relation to the PINO functional theory in Sec. II. In Sec. III we present the underlying assumptions of the ERPA and ERPA2 methods derived from the equations of motion of Rowe and we formulate time-dependent linear response APSG equations (TD-APSG). Then we discuss formal similarities and differences of the methods and their potential usefulness in obtaining single and double excitations at equilibrium and stretched-bond geometries. Applications to Li₂, BH, H₂O, and CH₂O molecules are presented in Sec. V. The paper is concluded in Sec. VI.

^{a)}Electronic mail: pernal@gmail.com

II. THE ANTISYMMETRIZED PRODUCT OF STRONGLY ORTHOGONAL GEMINAL FUNCTIONAL

Geminal theories are based on the ansatz for the wavefunction that employs the antisymmetrized product of two-electron functions called geminals. Imposing a strong orthogonality condition on geminals, i.e.,

$$\forall_{I \neq J} \forall_{\mathbf{x}_1, \mathbf{x}'_1} \int \psi_I(\mathbf{x}_1, \mathbf{x}_2) \psi_J(\mathbf{x}'_1, \mathbf{x}_2) d\mathbf{x}_2 = 0, \quad (1)$$

where I and J are indices of the geminals, leads to an approximation known as APSG. APSG has been a subject of extensive studies in the context of providing ground state energy of molecules.^{1,2,4,5} It is known that APSG is capable of predicting correct potential energy curves when one bond in a molecule is stretched, which is due to describing properly an interaction of electrons in a dissociating pair. The APSG curves are shifted upward with respect to the exact results that is attributed to the lack of dynamic correlation. The APSG expression for the energy in the representation of the natural orbitals reads

$$\begin{aligned} E^{APSG}[\{c_p\}, \{\varphi_p\}] &= 2 \sum_p c_p^2 h_{pp} + \sum_{pq} \delta_{I_p I_q} c_p c_q \langle pp|qq \rangle \\ &+ \sum_{pq} (1 - \delta_{I_p I_q}) c_p^2 c_q^2 [2\langle pq|pq \rangle - \langle pq|qp \rangle], \quad (2) \end{aligned}$$

where $\{\varphi_p(\mathbf{r})\}$ is a set of the APSG natural orbitals, which are real functions, the one- and two-electron integrals, $\{h_{pq}\}$ and $\{\langle pq|rs \rangle\}$, are in the representation of the natural orbitals, and I_p is the index of the geminal to which the p th orbital belongs to. The coefficients $\{c_p\}$ are directly related to the natural occupation numbers via the relation

$$\forall_p c_p^2 = n_p \quad (3)$$

(the natural occupation numbers $\{n_p\}$ are in the range $[0, 1]$). Due to the strong orthogonality condition, cf. Eq. (1), geminals are expanded in disjoint subsets (called Arai subspaces¹¹) of the natural orbitals and $\{c_p\}$ are the expansion coefficients, i.e.,

$$\begin{aligned} \forall_I \psi_I(\mathbf{x}_1, \mathbf{x}_2) &= 2^{-1/2} \sum_{p, I_p=I} c_p \varphi_p(\mathbf{r}_1) \varphi_p(\mathbf{r}_2) [\alpha(1)\beta(2) - \alpha(2)\beta(1)]. \quad (4) \end{aligned}$$

Normalization of each geminal implies

$$\forall_I \sum_{p, I_p=I} c_p^2 = 1. \quad (5)$$

For a two-electron molecule there is only one geminal so the third term in Eq. (2) that describes intergeminal electron interaction vanishes. Thus the total electron interaction is captured by the second term. This term describes exactly dissociation of a single electron pair. Its presence in the energy expression for systems consisting of more than two electrons leads to a correct qualitative behavior of the potential energy curves [cf. Ref. 5 and references cited therein]. It is due to the fact that two orbitals involved in bond breaking (i.e., those whose occupation numbers approach 1/2) belong

to the same geminal so their interaction is described by the intrageminal term. One can therefore say that the intrageminal term in the APSG energy expression is responsible for including the static correlation effects. The intergeminal term [the third term in Eq. (2)] includes only Coulomb and exchange interactions. Consequently, the interaction of orbitals belonging to different geminals misses correlation that is reflected in the upward shift of the potential energy curves.

Interestingly, since the expansion coefficients (3) can be written as products of phase factors and square roots of the occupation numbers, $c_p = \exp[2i\alpha_p] \sqrt{n_p}$, where $\alpha_p = 0$ or $\alpha_p = \pi/2$, one can write the APSG energy as a functional of the occupation numbers and the phase including natural orbitals $\{\pi_p\}$ defined as

$$\pi_p(\mathbf{r}) = \exp[i\alpha_p] \varphi_p(\mathbf{r}), \quad (6)$$

namely,

$$\begin{aligned} E^{APSG}[\{n_p\}, \{\pi_p\}] &= 2 \sum_p n_p h_{pp} + \sum_{pq} \delta_{I_p I_q} \sqrt{n_p n_q} \langle \pi_p \pi_p | \pi_q \pi_q \rangle \\ &+ \sum_{pq} \delta_{I_p I_q} n_p n_q [2\langle \pi_p \pi_q | \pi_p \pi_q \rangle - \langle \pi_p \pi_q | \pi_q \pi_p \rangle]. \quad (7) \end{aligned}$$

Clearly, there is no difference between the expressions given in Eqs. (2) and (7) when it comes to ground state calculation. However, Giesbertz *et al.* have recently formulated a time-dependent formalism for PINO functionals^{6,7,12} which can be readily applied to the APSG functional written in a PINO form, Eq. (7). We will return to this point in Sec. III.

III. EXTENDED RANDOM PHASE APPROXIMATIONS VERSUS TIME-DEPENDENT LINEAR RESPONSE THEORIES APPLIED TO APSG

As it has been already mentioned the APSG approximation is capable of capturing some static correlation effects present in ground states but at the same time it misses dynamical correlation. It is interesting to ask about performance of the APSG-based methods in obtaining excitation energies. Only recently some initial results have been presented.¹⁰ We briefly summarize two approaches, called ERPA and ERPA2, proposed in Ref. 10. They are based on the equations of motion of Rowe.¹³ Rowe's equations require defining the excitation operator. In ERPA such an operator includes only single excitations and the singlet operator reads

$$\begin{aligned} \hat{O}_{ERPA}^\dagger &= \sum_{p>q} X_{pq} (\hat{a}_{p\alpha}^\dagger \hat{a}_{q\alpha} + \hat{a}_{p\beta}^\dagger \hat{a}_{q\beta}) \\ &+ \sum_{p>q} Y_{pq} (\hat{a}_{q\alpha}^\dagger \hat{a}_{p\alpha} + \hat{a}_{q\beta}^\dagger \hat{a}_{p\beta}) \\ &+ \sum_p Z_p (\hat{a}_{p\alpha}^\dagger \hat{a}_{p\alpha} + \hat{a}_{p\beta}^\dagger \hat{a}_{p\beta}), \quad (8) \end{aligned}$$

where the creation and annihilation operators, $\hat{a}_{p\sigma}^\dagger$ and $\hat{a}_{p\sigma}$, respectively, act in the space of the natural spinorbitals. It has been shown that in case of singlet two-electron systems the ERPA excitation operator does not yield exact singlet

excited states.¹⁰ The problem is cured by including the diagonal double excitations in the operator that leads to the ERPA2 approximation

$$\begin{aligned} \hat{O}_{ERPA2}^\dagger = & \sum_{p>q} X_{pq} (\hat{a}_{p\alpha}^\dagger \hat{a}_{q\alpha} + \hat{a}_{p\beta}^\dagger \hat{a}_{q\beta}) \\ & + \sum_{p>q} Y_{pq} (\hat{a}_{q\alpha}^\dagger \hat{a}_{p\alpha} + \hat{a}_{q\beta}^\dagger \hat{a}_{p\beta}) \\ & + \sum_{pq} V_{pq} \hat{a}_{p\beta}^\dagger \hat{a}_{q\beta} \hat{a}_{p\alpha}^\dagger \hat{a}_{q\alpha}. \end{aligned} \quad (9)$$

Using the ERPA or ERPA2 excitation operators in the Rowe's equations leads to obtaining linear equations that employ one- and two-electron ground state reduced density matrices. Employing the reduced density matrices resulting from minimization of the APSG energy functional (2) yields the following ERPA equation:

$$\begin{pmatrix} \mathbf{0} & \mathbf{A}^- & \mathbf{0} \\ \mathbf{A}^+ & \mathbf{0} & \mathbf{D}^+ \\ 2(\mathbf{D}^+)^T & \mathbf{0} & \mathbf{E}^+ \end{pmatrix} \begin{pmatrix} \tilde{\mathbf{X}} \\ \tilde{\mathbf{Y}} \\ \tilde{\mathbf{Z}} \end{pmatrix} = \omega \begin{pmatrix} \tilde{\mathbf{X}} \\ \tilde{\mathbf{Y}} \\ \mathbf{0} \end{pmatrix}, \quad (10)$$

where

$$\forall_{p>q} \tilde{X}_{pq} = (c_p + c_q)(X_{pq} + Y_{pq}), \quad (11)$$

$$\forall_{p>q} \tilde{Y}_{pq} = (c_p - c_q)(Y_{pq} - X_{pq}), \quad (12)$$

$$\forall_p \tilde{Z}_p = 4c_p Z_p, \quad (13)$$

and the matrices \mathbf{A}^+ , \mathbf{A}^- , \mathbf{D}^+ , and \mathbf{E}^+ are determined by the optimal natural orbitals and the expansion coefficients $\{c_p\}$ and their elements read

$$\forall_{\substack{p>q \\ r>s}} A_{pq,rs}^+ = (c_p + c_q)^{-1}(A_{pq,rs} + B_{pq,rs})(c_r + c_s)^{-1}, \quad (14)$$

$$\forall_{\substack{p>q \\ r>s}} A_{rs,pq}^- = (c_p - c_q)^{-1}(A_{pq,rs} - B_{pq,rs})(c_r - c_s)^{-1}, \quad (15)$$

$$\forall_{p>r} D_{pq,r}^+ = \frac{B_{pq,rr}}{2(c_p + c_q)c_r}, \quad (16)$$

$$\forall_{pq} E_{pq}^+ = \frac{B_{pp,qq}}{4c_p c_q} \quad (17)$$

(for definitions of the \mathbf{A} and \mathbf{B} matrices, see the Appendix). Solving Eq. (10) and finding eigenvalues ω provide approximations to the excitation energies. Similarly, by employing the operator (9) in the Rowe's equations of motion together with the APSG density matrices leads to the ERPA2 approximation governed by the following equation:

$$\begin{pmatrix} \mathbf{0} & \mathbf{A}^- & \mathbf{D}^+ \\ \mathbf{A}^+ & \mathbf{0} & \mathbf{D}^+ \\ 2(\mathbf{D}^+)^T & \mathbf{0} & \mathbf{E}^+ \end{pmatrix} \begin{pmatrix} \tilde{\mathbf{X}} \\ \tilde{\mathbf{Y}} \\ \tilde{\mathbf{V}} \end{pmatrix} = \omega \begin{pmatrix} \tilde{\mathbf{X}} \\ \tilde{\mathbf{Y}} \\ \tilde{\mathbf{V}} \end{pmatrix}. \quad (18)$$

The vector $\tilde{\mathbf{Z}}$ in the ERPA approximation is related to the diagonal single excitations [see Eqs. (8) and (13)]. Similarly, the vector $\tilde{\mathbf{V}}$ in the ERPA2 equations is a consequence of the

presence of the diagonal double excitations in the ERPA2 excitation operator, Eq. (9). In particular, it is a contraction of the double excitation coefficients $\{V_{pq}\}$ with the coefficients $\{c_p\}$, i.e.,

$$\forall_p \tilde{V}_p = \sum_q V_{pq} c_q. \quad (19)$$

For that reason we call the elements of the $\tilde{\mathbf{V}}$ vector diagonal doubles and the excitations with a significant contribution from this vector—diagonal double excitations. One should notice that the ERPA and ERPA2 approximations yield the same values of excitation energies for excitations that couple neither to $\tilde{\mathbf{Z}}$ nor to $\tilde{\mathbf{V}}$ vector, respectively. To see it more clearly consider an excitation that involves nonzero elements \tilde{X}_{pq} and \tilde{Y}_{pq} corresponding to orbitals p and q such that the direct product of their irreducible representations does not contain A_1 , i.e., $\Gamma_p \otimes \Gamma_q \notin A_1$. Then, by confronting the definition of the \mathbf{D}^+ matrix given in Eqs. (16) and (A2) one immediately concludes that the $D_{pq,r}^+$ elements vanish for all r . With the \mathbf{D}^+ matrix being zero the upper left block of the ERPA [Eq. (10)] and ERPA2 [Eq. (18)] matrices decouple from the lower right block and both approximations yield the same results. On the other hand, for excitations involving \tilde{X}_{pq} and \tilde{Y}_{pq} such that $\Gamma_p \otimes \Gamma_q \in A_1$ (in particular excitations to states of the A_1 symmetry) the ERPA and ERPA2 are expected to yield different results (cf. an analogical discussion presented in Ref. 14 concerning excitation energies of the H_2 molecule).

Both ERPA and ERPA2 approaches employing the APSG density matrices should be able to capture multireference character of excited states and they are expected to yield some excitations of a double character alongside the single excitations. There are two reasons for that. One of the reasons is that the APSG ground state wavefunction expanded into a sum of Slater determinants is of a multiconfigurational nature. Thus, acting on such a wavefunction even with the ERPA excitation operator, Eq. (8), that includes only single excitations, may result in obtaining double excitations. Indeed, as shown in Ref. 10 the first 1D excitation of beryllium which is considered to be a pure double excitation is very accurately described by both ERPA and ERPA2. On the other hand, the $^1\Sigma_g^+$ double excitation of the hydrogen molecule is missing in ERPA since it would require a double excitation component in the excitation operator that ERPA misses. ERPA2, on the other hand, should be more effective in reproducing excitations of a double character since not only it is based on the multiconfigurational APSG ground state but also it explicitly includes double excitations in the underlying excitation operator given in Eq. (9). Evidently, ERPA2 operator does not include all double excitations but only the diagonal ones. Their presence will have an effect only on some excitations and some double excitations may be missing as it will be shown in Sec. V.

A question arises if one can formulate a time-dependent linear response theory with the APSG wavefunction and if it would bring an improvement to the ERPA approaches. We start by writing the quantum action integral for the time-dependent APSG wavefunction. Assuming that partitioning of space of the time-dependent orbitals into geminals stays

invariant in time (an assignment of a given orbital to a geminal does not change in time, i.e., the indices $\{I_p\}$ are fixed) one obtains

$$\begin{aligned}
A &= \int_0^T \left\langle \Psi^{APSG}(t) | \hat{H}(t) - i \frac{\partial}{\partial t} | \Psi^{APSG}(t) \right\rangle dt \\
&= 2 \sum_p \int_0^T c_p(t)^* c_p(t) h_{pp}(t) dt \\
&\quad + \sum_{\substack{p,q \\ I_p = I_q}} \int_0^T c_p^*(t) c_q(t) \langle p(t)p(t) | q(t)q(t) \rangle dt \\
&\quad + \sum_{\substack{p,q \\ I_p \neq I_q}} \int_0^T n_p(t) n_q(t) \langle p(t)q(t) | p(t)q(t) \rangle dt \\
&\quad - i \sum_p \int_0^T [c_p(t)^* \dot{c}_p(t) + 2c_p(t)^* c_p(t) \langle p(t) | \dot{p}(t) \rangle] dt,
\end{aligned} \tag{20}$$

where all integrals employ time-dependent natural orbitals $\{\varphi_p(\mathbf{r}, t)\}$ and expansion coefficients $\{c_p(t)\}$ [cf. Eq. (4)], and the Hamiltonian includes the kinetic part, the electron-electron interaction operator, and the time-dependent external potential, namely,

$$\hat{H}(t) = \hat{T} + \hat{V}_{ee} + \hat{V}_{ext}(t). \tag{21}$$

The two-electron integrals are defined as follows:

$$\begin{aligned}
\langle p(t)q(t) | r(t)s(t) \rangle \\
= 2 \langle p(t)q(t) | r(t)s(t) \rangle - \langle p(t)q(t) | s(t)r(t) \rangle,
\end{aligned} \tag{22}$$

$$\begin{aligned}
\langle p(t)q(t) | r(t)s(t) \rangle \\
= \iint \varphi_p(\mathbf{r}_1, t)^* \varphi_q(\mathbf{r}_2, t)^* |\mathbf{r}_1 - \mathbf{r}_2|^{-1} \varphi_r(\mathbf{r}_1, t) \varphi_s(\mathbf{r}_2, t) d\mathbf{r}_1 d\mathbf{r}_2.
\end{aligned} \tag{23}$$

The time-dependent linear response APSG equations can be obtained in a straightforward manner by exploiting stationarity of the action and by employing standard linear response theory. Notice that since the APSG functional is a special case of the PINO functional, cf. Eq. (7), one can immediately adopt linear response PINO equations presented in Refs. 6 and 7. Since all steps of the derivation have been already provided in Ref. 7 there is no need to repeat them here and we only provide a final form of the linear response APSG equations that read

$$\forall_p \quad \omega P_{pp}^{\text{Re}}(\omega) = 2 \sum_{q>r} (D^+)^T_{p,qr} P_{qr}^{\text{Im}}(\omega) + \sum_q E_{pq}^+ P_{qq}^{\text{Im}}(\omega), \tag{24}$$

$$\begin{aligned}
\forall_p \quad \omega P_{pp}^{\text{Im}}(\omega) &= 2 \sum_{q>r} (D^-)^T_{p,qr} P_{qr}^{\text{Re}}(\omega) \\
&\quad + \sum_q E_{pq}^- P_{qq}^{\text{Re}}(\omega) + 2c_p v_{pp}^{\text{Re}}(\omega),
\end{aligned} \tag{25}$$

$$\begin{aligned}
\forall_{p>q} \quad \omega P_{pq}^{\text{Re}}(\omega) &= \sum_{r>s} A_{pq,rs}^+ P_{rs}^{\text{Im}}(\omega) \\
&\quad + \sum_r D_{pq,r}^+ P_{rr}^{\text{Im}}(\omega) + (c_p - c_q) v_{qp}^{\text{Im}}(\omega),
\end{aligned} \tag{26}$$

$$\begin{aligned}
\forall_{p>q} \quad \omega P_{pq}^{\text{Im}}(\omega) &= \sum_{r>s} A_{pq,rs}^- P_{rs}^{\text{Re}}(\omega) \\
&\quad + \sum_r D_{pq,r}^- P_{rr}^{\text{Re}}(\omega) + (c_q + c_p) v_{qp}^{\text{Re}}(\omega).
\end{aligned} \tag{27}$$

We use a notation $f^{\text{Re}}(\omega)$ and $f^{\text{Im}}(\omega)$ for the Fourier transforms of the real and imaginary parts of $\delta f(t)$ (the first-order perturbation to the quantity f), the imaginary part being multiplied by the imaginary unit i , i.e.,

$$f^{\text{Re}}(\omega) = \mathcal{F}[\text{Re } \delta f(t)](\omega), \tag{28}$$

$$f^{\text{Im}}(\omega) = i \mathcal{F}[\text{Im } \delta f(t)](\omega). \tag{29}$$

The first-order perturbations to the natural orbitals have been expanded in the basis of the stationary orbitals, namely,

$$\varphi_p(\mathbf{r}, \omega) = \sum_q \delta U_{pq}(\omega) \varphi_q(\mathbf{r}), \tag{30}$$

and the matrices $\mathbf{P}^{\text{Re/Im}}(\omega)$ present in Eqs. (24)–(27) are the first-order perturbations to the matrix $\mathbf{P} = \mathbf{UcU}$ whose components read

$$\forall_{pq} \quad P_{pq}^{\text{Re}}(\omega) = \delta_{pq} c_p^{\text{Re}}(\omega) + (c_p - c_r) U_{pq}^{\text{Re}}(\omega), \tag{31}$$

$$\forall_{pq} \quad P_{pq}^{\text{Im}}(\omega) = \delta_{pq} c_p^{\text{Im}}(\omega) + (c_p + c_q) U_{pq}^{\text{Im}}(\omega). \tag{32}$$

The matrices \mathbf{A}^+ , \mathbf{A}^- , \mathbf{D}^+ , and \mathbf{E}^+ have been already encountered in the ERPA2 equations and their elements are given in Eqs. (14)–(17) and (A1)–(A3). Definitions of \mathbf{D}^- and \mathbf{E}^- matrices that do not have the counterparts in the ERPA2 equations are explicitly shown in the Appendix [see Eqs. (A5) and (A6)]. Excitation energies follow as singularities of the linear response matrix and they are found by solving the equations (Eqs. (24)–(27)) with the perturbation $v(\omega)$ set to zero. Thus, the APSG linear response equations that provide excitation energies as eigenvalues read

$$\begin{pmatrix} \mathbf{0} & \mathbf{A}^- & \mathbf{0} & \mathbf{D}^- \\ \mathbf{A}^+ & \mathbf{0} & \mathbf{D}^+ & \mathbf{0} \\ \mathbf{0} & 2(\mathbf{D}^-)^T & \mathbf{0} & \mathbf{E}^- \\ 2(\mathbf{D}^+)^T & \mathbf{0} & \mathbf{E}^+ & \mathbf{0} \end{pmatrix} \begin{pmatrix} \tilde{\mathbf{X}} \\ \tilde{\mathbf{Y}} \\ \tilde{\mathbf{V}} \\ \tilde{\mathbf{W}} \end{pmatrix} = \omega \begin{pmatrix} \tilde{\mathbf{X}} \\ \tilde{\mathbf{Y}} \\ \tilde{\mathbf{V}} \\ \tilde{\mathbf{W}} \end{pmatrix}. \tag{33}$$

We use the abbreviation TD-APSG for the method based on Eq. (33). One should notice here that the derived response equations are different from the coupled perturbed APSG equations proposed in Ref. 9. The $\tilde{\mathbf{X}}$ and $\tilde{\mathbf{Y}}$ vectors present there pertain to excitations between occupied and virtual geminals that are expanded in the same Arai subspaces of one-electron functions. In Eq. (33) the vectors $\tilde{\mathbf{X}}$ and $\tilde{\mathbf{Y}}$ pertain to pairs of orbitals belonging to the same or different Arai subspaces. Even though no results have been presented one

expects that the formalism proposed in Ref. 9 will lack diagonal double excitations and, due to including only excitations involving orbitals belonging to the same Arai subspaces, excitation energies requiring intergeminal contributions will be deficient.

A comparison of the TD-APSG equations with that of ERPA, Eq. (10), shows immediately that they differ. So unlike the linear response Hartree-Fock equations (TD-HF) that are equivalent to the RPA (random phase approximation) method, the linear response APSG approach does not lead to the same equations as the Rowe's equation of motion taken with single excitation operators [cf. Eq. (8)] and the APSG ground state. TD-APSG is not fully equivalent to ERPA2 either. However, for excitations that do not couple to the vectors $\tilde{\mathbf{V}}$ and

$\tilde{\mathbf{W}}$ the elements of the matrices \mathbf{D}^+ and \mathbf{D}^- in Eq. (33) vanish [cf. a discussion on equivalence of ERPA and ERPA2 below Eq. (19)] and all three approximations: TD-APSG, ERPA, and ERPA2 yield the same excitation energies. As it has been mentioned in Ref. 10 solving the ERPA2 equations provides negative and positive values of ω that for excitations coupling to $\tilde{\mathbf{V}}$ do not show a sign symmetry. In other words, a positive value ω is not accompanied by a negative ω of the same absolute value. Only those ERPA2 excitation energies that do not couple to the $\tilde{\mathbf{V}}$ vector come in positive/negative-value pairs. Eigenvalues of the TD-APSG equations, on the other hand, come in pairs regardless of their symmetry. This is clearly seen if Eq. (33) is written in an equivalent form

$$\begin{pmatrix} \mathbf{A}^+\mathbf{A}^- + 2\mathbf{D}^+(\mathbf{D}^-)^T & \mathbf{A}^+\mathbf{D}^- + \mathbf{D}^+\mathbf{E}^- \\ 2[(\mathbf{D}^+)^T\mathbf{A}^- + \mathbf{E}^+(\mathbf{D}^-)^T] & 2(\mathbf{D}^+)^T\mathbf{D}^- + \mathbf{E}^+\mathbf{E}^- \end{pmatrix} \begin{pmatrix} \tilde{\mathbf{Y}} \\ \tilde{\mathbf{W}} \end{pmatrix} = \omega^2 \begin{pmatrix} \tilde{\mathbf{Y}} \\ \tilde{\mathbf{W}} \end{pmatrix} \quad (34)$$

obtained by eliminating the $\tilde{\mathbf{X}}$ and $\tilde{\mathbf{V}}$ vectors and reducing the dimension of the main matrix by a factor 2. Even though for the diagonal double excitations the TD-APSG and ERPA2 approaches are governed by non-equivalent equations, it will be shown in Sec. V that numerically the excitation energies obtained from both methods are very close. To understand when the two methods are expected to yield similar results for excitations that include diagonal doubles, i.e., for those that couple to the vectors $\tilde{\mathbf{V}}$ in case of ERPA2 and $\tilde{\mathbf{W}}$ in case of TD-APSG consider an example of the excitation that involves only intrageminal contributions. This means that the nonzero elements of the vectors $\tilde{\mathbf{X}}$ and $\tilde{\mathbf{Y}}$ include only those that pertain to the same geminal, say I , i.e., $\forall_{p>q} \tilde{X}_{pq}, \tilde{Y}_{pq} \neq 0 \Rightarrow I_p = I_q = I$. Then it can be shown that the matrices with the “+” subscript are the same as their counterparts subscripted with “-,” namely,

$$\forall_I \quad \forall_{p>q, I_p=I_q=I} \quad A_{pq,rs}^+ = A_{pq,rs}^-, \quad (35)$$

$$\forall_I \quad \forall_{p>q, I_p=I_q=I} \quad D_{pq,r}^+ = D_{pq,r}^-, \quad (36)$$

$$\forall_I \quad \forall_{p,q, I_p=I_q=I} \quad E_{pq}^+ = E_{pq}^-. \quad (37)$$

By inspection one checks that a solution to the TD-APSG eigenproblem with an excitation energy ω_n^+ and the vectors satisfying equations $\tilde{\mathbf{X}}_n = \tilde{\mathbf{Y}}_n$, $\tilde{\mathbf{V}}_n = \tilde{\mathbf{W}}_n$, and

$$\mathbf{A}^+\tilde{\mathbf{X}}_n + \mathbf{D}^+\tilde{\mathbf{V}}_n = \omega_n^+\tilde{\mathbf{X}}_n, \quad (38)$$

$$2(\mathbf{D}^+)^T\tilde{\mathbf{X}}_n + \mathbf{E}^+\tilde{\mathbf{V}}_n = \omega_n^+\tilde{\mathbf{V}}_n, \quad (39)$$

is accompanied by a counterpart solution such that $\omega_n^- = -\omega_n^+$, $\tilde{\mathbf{X}}_n = -\tilde{\mathbf{Y}}_n$, $\tilde{\mathbf{V}}_n = -\tilde{\mathbf{W}}_n$. It can be immediately confirmed by looking at the ERPA2 equations (18) that for the entirely intrageminal excitations [for which Eqs. (35)–(37) hold] the vectors $\tilde{\mathbf{X}}_n = -\tilde{\mathbf{Y}}_n$, $\tilde{\mathbf{V}}_n$ obtained from TD-APSG

equations (38) and (39) satisfy also the ERPA2 equations with the eigenvalue ω_n^+ . The positive solutions of TD-APSG are therefore identical to the positive solutions of ERPA2 in case of intrageminal excitations. It is not the case with the negative solutions, however. To summarize, we have shown that in case of excitations not coupling the diagonal doubles all three considered approximations ERPA, ERPA2, and TD-APSG yield identical results. For excitations coupling to the diagonal doubles (involving the nonzero vectors $\tilde{\mathbf{V}}$ and $\tilde{\mathbf{W}}$) the positive solutions to the TD-APSG and ERPA2 equations are expected to be close for excitations dominated by the intrageminal contributions.

It has been elucidated in Sec. II that the APSG expression for the energy, Eq. (2), can be viewed as an example of the phase including natural orbital (PINO) functional [cf. Eq. (7)]. The PINO theory has been developed recently by Giesbertz *et al.* in the context of computing excitation energies in the adiabatic PINO approximation.^{6,7} The linear response PINO equations presented in Ref. 7 employ as variables a response of the one-electron reduced density matrix $\gamma(\omega)$ and, additionally, a response of phases of PINO's, $\{\tilde{U}_{pp}^{\text{Im}}(\omega)\}$, where $\pi_p(\mathbf{r}, \omega) = \sum_q \tilde{U}_{pq}(\omega)\pi_q(\mathbf{r})$ [cf. Eq. (6)]. Comparison of the PINO equations based on the APSG functional (7) and the TD-APSG equations [Eqs. (24)–(27)] is immediately afforded by noticing the following relations:

$$\forall_{p>q} \quad (c_p + c_q)P_{pq}^{\text{Re}}(\omega) = \gamma_{pq}^{\text{Re}}(\omega), \quad (40)$$

$$\forall_{p>q} \quad (c_q - c_p)P_{pq}^{\text{Im}}(\omega) = \gamma_{pq}^{\text{Im}}(\omega), \quad (41)$$

$$\forall_p \quad 2c_p P_{pp}^{\text{Re}}(\omega) = \gamma_{pp}^{\text{Re}}(\omega) = n_p(\omega), \quad (42)$$

$$\forall_p \quad (2c_p)^{-1} P_{pp}^{\text{Im}}(\omega) = \tilde{U}_{pp}^{\text{Im}}(\omega). \quad (43)$$

Therefore, for excitations of mainly intrageminal character, for which TD-APSG excitation energies and the positive solutions of the ERPA2 approach are expected to be very close, the vector $\tilde{\mathbf{V}}$ present in ERPA2 equations (18) becomes equal to $\mathbf{n}(\omega)$ —a response of the occupation numbers. Taking into account Eqs. (9) and (19) it is evident that since $\tilde{\mathbf{V}}$ is directly linked to the presence of the diagonal excitation operators then the nonzero elements of the $\mathbf{n}(\omega)$ vector indicate a double character of a pertinent excitation. This fact has been already anticipated in Ref. 14 based on the observation of a nonzero contribution of the $\mathbf{n}(\omega)$ elements to the double $^1\Sigma_g^+$ excitation of the H_2 molecule.

Formulation of the time-dependent linear response theory for the APSG wavefunction opens avenue to a possible improvement of the accuracy of the TD-APSG method in predicting single excitations by exploiting the idea of range-separating the electron-electron interaction operator. The idea was first introduced by Savin in order to improve description of ground states by approximate density functional theory (DFT).¹⁵ The range-separation concept leads to new functionals that employ both a wavefunction (usually of a multiconfigurational character) in the description of the long-range regime of the electron-electron interaction and a short-range density functional. The central assumption in the range-separation methods is to split the electron-electron interaction into the short- and long-range components, $r_{12}^{-1} = v_{ee,\mu}^{LR}(r_{12}) + v_{ee,\mu}^{SR}(r_{12})$, where $\lim_{r_{12} \rightarrow \infty} r_{12} v_{ee,\mu}^{LR}(r_{12}) = \lim_{r_{12} \rightarrow 0} r_{12} v_{ee,\mu}^{SR}(r_{12}) = 1$. The parameter μ that governs the partitioning is such that $\lim_{\mu \rightarrow \infty} v_{ee,\mu}^{LR}(r_{12}) = \lim_{\mu \rightarrow 0} v_{ee,\mu}^{SR}(r_{12}) = r_{12}^{-1}$. Only very recently, the idea of range-separation has been extended to embrace time-dependent systems, which has led to methods combining short-range exchange-correlation DFT kernels with the long-range multiconfiguration¹⁶ or single determinantal¹⁷ wavefunction approaches or with the long-range density matrix functionals.¹⁸ It has been argued in Refs. 18 and 16 that adding a long-range component of a multiconfigurational character to the DFT kernel (restricted to the short-range regime) offers an improvement over DFT in description of double and charge transfer excitations. On the other hand, since adiabatic approximation TD-DFT methods are usually quite satisfactory in describing low-lying single excitations, including the short-range DFT kernels in the time-dependent wavefunction (or density matrix functional) approaches is expected to improve the accuracy of such excitations (in case of the MC-SCF method it should be achieved with a modest size of the configuration space).

In order to employ the range-separation approach in the time-dependent strongly orthogonal geminal description of a system, the Hamiltonian present in the quantum action given in Eq. (20) is modified to include the long-range electron-electron interaction and a time-dependent potential $V_\mu^{SR}(t)$ (called a short-range potential), namely,

$$\hat{H}_\mu(t) = \hat{T} + \hat{V}_{ee,\mu}^{LR} + \hat{V}_{ext}(t) + V_\mu^{SR}(t). \quad (44)$$

In principle, the short-range potential should be defined in such a way that the exact density is recovered.¹⁸ Since the wavefunction is restricted to be of the APSG form such a

potential probably does not exist in general, and one has to resort to approximations. The most popular and convenient (from the perspective of computation of two-electron integrals) choice of the long-range electron-electron interaction operator employs the error function, i.e.,

$$\hat{V}_{ee,\mu}^{LR} = \sum_{i < j}^N \frac{\text{erf}(r_{ij}\mu)}{r_{ij}}. \quad (45)$$

Having defined the Hamiltonian the derivation of the range-separated linear response equations proceeds in a similar way as derivation of Eqs. (24)–(27), the difference being in the fact that the perturbing potential is now a sum of the external potential $\delta v(t)$ and the response of the short-range potential, $\delta v_\mu^{SR}(t)$. Consequently, the linear response theory in the adiabatic approximation leads to equations of the same structure as Eqs. (24)–(27), i.e., the time-dependent long-range-APSG (TD-IrAPSG) equations take form

$$\begin{pmatrix} \mathbf{0} & \mathbf{A}_\mu^- & \mathbf{0} & \mathbf{D}_\mu^- \\ \mathbf{A}_\mu^+ & \mathbf{0} & \mathbf{D}_\mu^+ & \mathbf{0} \\ \mathbf{0} & 2(\mathbf{D}_\mu^-)^T & \mathbf{0} & \mathbf{E}_\mu^- \\ 2(\mathbf{D}_\mu^+)^T & \mathbf{0} & \mathbf{E}_\mu^+ & \mathbf{0} \end{pmatrix} \begin{pmatrix} \tilde{\mathbf{X}} \\ \tilde{\mathbf{Y}} \\ \tilde{\mathbf{V}} \\ \tilde{\mathbf{W}} \end{pmatrix} = \omega \begin{pmatrix} \tilde{\mathbf{X}} \\ \tilde{\mathbf{Y}} \\ \tilde{\mathbf{V}} \\ \tilde{\mathbf{W}} \end{pmatrix}. \quad (46)$$

The matrices $\mathbf{A}_\mu^{+/-}$, $\mathbf{D}_\mu^{+/-}$, and $\mathbf{E}_\mu^{+/-}$ are defined in a similar way as the matrices \mathbf{A}^+ , \mathbf{D}^+ , and \mathbf{E}^+ but they involve two-electron integrals with the long-range operator, i.e.,

$$\langle pq|rs \rangle_\mu = \iint \varphi_p(\mathbf{r}_1)^* \varphi_q(\mathbf{r}_2)^* \frac{\text{erf}(r_{12}\mu)}{r_{12}} \varphi_r(\mathbf{r}_1) \varphi_s(\mathbf{r}_2) d\mathbf{r}_1 d\mathbf{r}_2, \quad (47)$$

and the one-electron Hamiltonian elements include a contribution from the short-range potential

$$h_{pq}^\mu = \langle p|\hat{t} + \hat{v}_{ext} + v_\mu^{SR}[\rho]|q \rangle, \quad (48)$$

where $v_\mu^{SR}[\rho]$ is a derivative of the employed short-range density functional (that includes a short-range Hartree, exchange, and correlation components)

$$v_\mu^{SR}[\rho](\mathbf{r}) = \frac{\delta E_\mu^{SR}[\rho]}{\delta \rho(\mathbf{r})}. \quad (49)$$

Additionally, the matrices \mathbf{A}_μ^- , \mathbf{D}_μ^- , and \mathbf{E}_μ^- include contributions from a short-range density kernel

$$K_{pqrs}^{SR} = \iint \varphi_p(\mathbf{r}_1)^* \varphi_q(\mathbf{r}_2)^* \frac{\delta^2 E_\mu^{SR}[\rho]}{\delta \rho(\mathbf{r}_1) \delta \rho(\mathbf{r}_2)} \varphi_r(\mathbf{r}_1) \varphi_s(\mathbf{r}_2) d\mathbf{r}_1 d\mathbf{r}_2. \quad (50)$$

The complete definitions of the aforementioned matrices are presented in the Appendix.

IV. COMPUTATIONAL DETAILS

We apply the approaches described in Sec. III, i.e., ERPA, ERPA2, TD-APSG, and TD-IrAPSG to a number of molecules in order to investigate the capabilities of the methods to reproduce both single excitations and excitations of a double character at equilibrium geometries and in cases when one of the bonds is elongated. Equations governing all the methods employ one- and two-electron APSG reduced density matrices. They are obtained by optimizing the APSG

energy functional given in Eq. (2) with respect to the coefficients $\{c_p\}$ and the orbitals $\{\varphi_p\}$ with the orthonormality condition imposed on the latter and a sum rule, Eq. (5), on the former. We have adopted a two-step procedure already employed in the optimization of reduced density matrix functionals,¹⁹ i.e., in the first step of each macroiteration optimal coefficients are found for a given set of orbitals and subsequently the coefficients are fixed and the optimization with respect to orbitals is carried out. The APSG energy optimization should also take into account finding optimal geminal (Arai) subspaces. An efficient method that serves this purpose has been already proposed by Rassolov.⁴ We have adopted a simpler and less effective approach to the problem that still leads to smooth potential energy curves. Namely, for given sets of the APSG orbitals $\{\varphi_p\}$ and geminal-assignment indices $\{I_p\}$ it is checked if moving an orbital p from a geminal I_p to J and carrying out optimization of all coefficients $\{c_p\}$ lowers the energy. If it does the new assignment is saved. Such a procedure is conducted for all geminals J and all orbitals p . Since the orbitals obtained from optimization of the APSG functional are subsequently used to find excitation energies they are symmetry-constrained. Using symmetrized orbitals leads, on one hand, to higher ground state energies than that obtained with the localized orbitals but on the other hand it allows for symmetry assignment of excitations. Another argument that justifies the usage of symmetry-constrained orbitals is the fact that, formally, the ERPA and TD-PINO equations (TD-APSG being a special case of the latter) employ natural orbitals. Natural orbitals are delocalized and of certain symmetries so approximate orbitals employed in calculations should possess the same features. We have checked that differences in excitation energies obtained either with symmetry-constrained or localized orbitals range from 0.0 to 0.4 eV for CH₂O and H₂O molecules.

The density matrices employed in the range-separated TD-IrAPSG approximation [cf. Eqs. (46)–(50)] result from minimizing a range-separated APSG functional E_μ^{APSG} which employs the long-range electron-electron interaction operator in two-electron integrals $\langle pq|rs\rangle_\mu$ [cf. Eq. (47)] and the short-range density functional $E_\mu^{SR}[\rho]$, i.e.,

$$\begin{aligned} E_\mu^{APSG}[\{c_p\}, \{\varphi_p\}] &= 2 \sum_p c_p^2 h_{pp} + \sum_{pq} \delta_{I_p I_q} c_p c_q \langle pp|qq\rangle_\mu \\ &+ \sum_{pq} (1 - \delta_{I_p I_q}) c_p^2 c_q^2 (2 \langle pq|pq\rangle_\mu - \langle pq|qp\rangle_\mu) + E_\mu^{SR}[\rho]. \end{aligned} \quad (51)$$

In our actual calculations the density functional $E_\mu^{SR}[\rho]$ is approximated by the short-range local density approximation (SR-LDA) functional proposed in Ref. 20. This functional is utilized in both ground state energy optimization [Eq. (51)] and the excitation energy calculations [via the short-range kernel, Eq. (50)]. In all calculations with the range-separated methods we have used one value of the parameter μ equal to 0.4 a.u.

In order to find excitation energies within the ERPA, ERPA2, TD-APSG, and TD-IrAPSG method one solves a per-

tinuous eigenproblem given, respectively, in Eqs. (10), (18), (33), and (46). The matrices entering all eigenproblems involve divisions by sums and differences of two coefficients, $c_p \pm c_q$ [cf. Eqs. (14)–(16) and (A5)]. We have observed that occasionally there were unphysical excitation energies found among the first few physical ones. The composition of the spurious excitations is dominated by pairs of orbitals φ_p and φ_q the occupation numbers of which are either very low (both close to 0) or very high (both close to 1). The appearance of the spurious excitations can be eliminated by removing from the $\tilde{\mathbf{X}}$ and $\tilde{\mathbf{Y}}$ vectors the elements \tilde{X}_{pq} and \tilde{Y}_{pq} corresponding to the “faulty” pairs. In all our calculations we have assumed the lower and upper cutoffs for sums of pairs of occupation numbers that are included in calculations. In other words, the accepted elements of the vectors $\tilde{\mathbf{X}}$ and $\tilde{\mathbf{Y}}$ are such that $\forall_{p>q} 1 \times 10^{-4} > n_p + n_q > 1.98$ (only for H₂O molecule with the TD-IrAPSG method the upper limit has been lowered to 1.8). We have checked that the effect of changing the cutoffs on the physical excitation energies is of the order of 10^{-2} eV.

We have investigated performance of the afore described methods for predicting excitation energies of Li₂, BH, H₂O, and CH₂O molecules at both equilibrium and, in case of the first three species, at stretched bond geometries. For Li₂ cc-pVTZ²¹ basis set was used, whereas formaldehyde calculations were performed in the TZVP basis.²² For BH and H₂O we employed modified augmented cc-pVDZ basis sets proposed in Refs. 23 and 24, respectively. The equilibrium bond lengths for the Li₂ and BH molecules assumed in calculations read, respectively, $R_{eq} = 5.052$ a.u. and $R_{eq} = 2.329$ a.u. Geometries for H₂O, and CH₂O molecules are taken from Refs. 24 and 25, respectively. The APSG excitations are compared with those obtained by employing the coupled-cluster single double (CCSD) (equation of motion coupled cluster singles doubles) and RPA (equivalent to TD-HF) methods for which dalton suite of programs has been employed.²⁶

V. RESULTS

The results of ERPA, ERPA2, and TD-APSG calculations on molecules at equilibrium geometries are presented in Tables I and II. Additionally, in Figs. 1–5 we show excitation energy curves obtained for dissociating molecules. Since in all investigated cases the TD-APSG excitation energies parallel very closely those of ERPA2 the differences would be

TABLE I. Singlet excitation energies in eV for Li₂ and BH molecules at equilibrium bond lengths.

Molecule	State	CCSD	RPA	ERPA	ERPA2	TD-APSG
Li ₂	2 ¹ Σ _g ⁺	2.73	2.92	3.03	2.69	2.71
	3 ¹ Σ _g ⁺	4.17	4.63	4.80	4.17	4.23
	1 ¹ Σ _u ⁺	1.85	2.08	1.84	1.84	1.84
	1 ¹ Δ _g	4.11	—	4.20	4.20	4.20
BH	2 ¹ Σ ⁺	6.42	6.36	6.80	6.71	6.69
	4 ¹ Σ ⁺	7.76	7.38	7.77	7.72	7.72
	1 ¹ Δ	6.67	—	9.39	9.39	9.39
	2 ¹ Δ	8.33	8.08	8.24	8.24	8.24

TABLE II. Singlet excitation energies in eV for H₂O and CH₂O molecules at equilibrium geometries.

Molecule	State	CCSD	RPA	TD-APSG	TD-IrAPSG
H ₂ O	1 ¹ B ₁	7.38	8.63	8.54	7.43
	1 ¹ A ₂	9.12	10.32	10.21	9.08
	2 ¹ A ₁	9.81	10.95	10.81	9.51
	1 ¹ B ₂	11.52	12.61	12.50	11.17
CH ₂ O	1 ¹ A ₂	3.97	4.28	4.36	3.84
	1 ¹ B ₂	8.45	10.15	10.32	8.76
	1 ¹ B ₁	9.26	9.36	8.90	9.10
	2 ¹ A ₁	9.77	9.16	9.61	9.61

invisible on the plots so either ERPA2 or TD-APSG curves are shown in figures. The APSG results are compared with those obtained with the CCSD method. For cases when reliability of the CCSD excitation energies is in question we have also included results obtained from the CC3 model that includes triples amplitudes and is an approximation to the CCSDT approach.²⁷ We also present excitation energies following from RPA to show the effects of (i) using a correlated APSG ground state wavefunction instead of a single determinant as it is done in RPA and (ii) including diagonal double terms in ERPA2 and TD-APSG instead of only off-diagonal single excitations included in RPA.

Following a discussion presented in Refs. 28 and 18 on how to identify double excitations based on the composition of the \tilde{X} , \tilde{Y} vectors and also noting a straightforward relation of the elements of the \tilde{V} vector [Eq. (19)] with the diagonal double excitations present in the ERPA2 operator it can be assumed that a double character of a given excitation is identified by the presence of nonzero elements of the \tilde{V} or \tilde{W} vectors and/or nonzero elements \tilde{X}_{pq} , \tilde{Y}_{pq} for which both indices p and q correspond to strongly or weakly occupied orbitals, $n_p, n_q > 1/2$ or $n_p, n_q < 1/2$, respectively.

The data present in Table I and Fig. 1 for the Li₂ molecule confirm that since the 1¹Σ_g⁺ excitations couple to diagonal double elements \tilde{V} the ERPA2 results for this symmetry differ

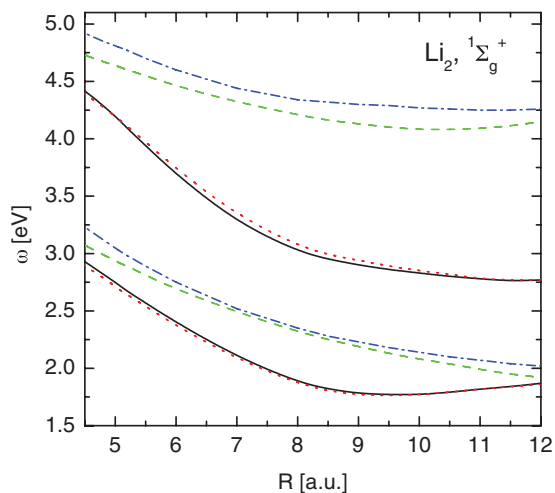


FIG. 1. Potential energy curves of the first 1¹Σ_g⁺ excited states for the dissociating Li₂ molecule. Solid lines: CCSD, dotted lines: ERPA2, dashed-dotted lines: ERPA, and dashed lines: RPA results.

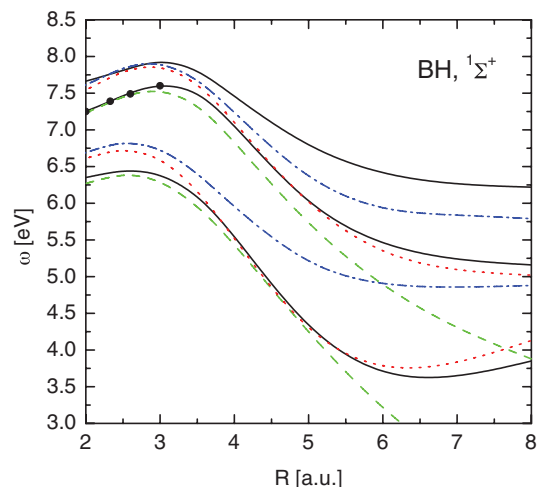


FIG. 2. Potential energy curves of the first 1¹Σ⁺ excited states for the dissociating BH molecule. Solid lines: CCSD, dotted lines: ERPA2, dashed-dotted lines: ERPA, and dashed lines: RPA results. Dots indicate a double excitation character of the second CCSD excitation.

from those of ERPA. On the other hand, for excitations of all symmetries ERPA2 and TD-APSG excitations are almost the same (within 0.06 eV). This has been expected based on the arguments provided in Sec. III [cf. Eqs. (35)–(37)], since all Li₂ excitations are dominated by intrageminal contributions. Looking at the results in Table I and Fig. 1 one concludes that the importance of treating diagonal contributions properly is even greater than the need to use a correlated wavefunction. Namely, the error of the ERPA excitations exceeds that of the RPA for all interatomic distances R . The deviations of the two methods from CCSD are larger for the excitation to the 3¹Σ_g⁺ state than to 2¹Σ_g⁺, which is due to a stronger double character of the former. At equilibrium geometry the 3¹Σ_g⁺ state includes 2σ_g² → 3σ_g² and 2σ_g² → 2σ_u² double excitations and a proper treatment of diagonal double elements, missing in ERPA, is necessary. Apparently, ERPA2 (and TD-APSG)

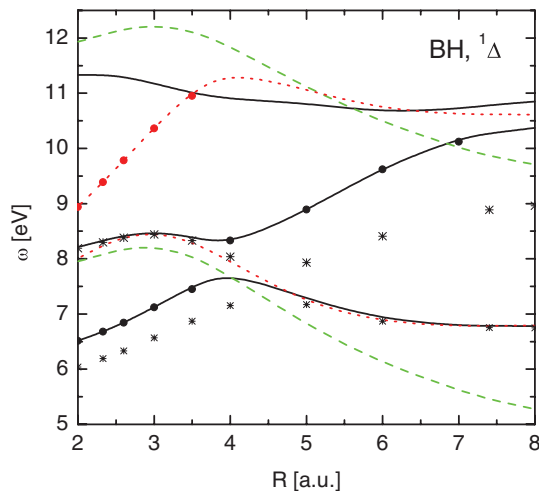


FIG. 3. Potential energy curves of the first 1¹Δ excited states for the dissociating BH molecule. Solid lines: CCSD, asterisks: CC3, dotted lines: ERPA2 (equivalent to ERPA2 and TD-APSG for the considered excitations), and dashed lines: RPA results. Dots indicate a double excitation character of the CCSD and ERPA excitations.

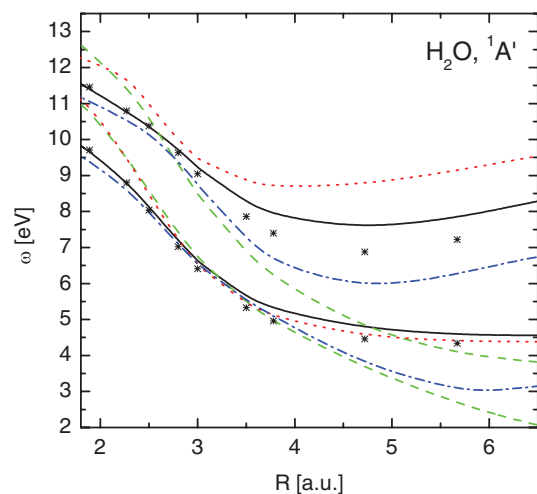


FIG. 4. Potential energy curves of the $1A'$ excited states for the H_2O molecule with one dissociating bond. Solid lines: CCSD, asterisks: CC3, dotted lines: TD-APSG, dashed-dotted: TD-lrAPSG, and dashed lines: RPA results.

excitations are in a good agreement with the CCSD references in the whole range of interatomic distances R for all shown $1\Sigma_g^+$ states. The $1^1\Delta_g$ excitation of Li_2 is a pure double one that can be described in the orbital picture as a $2\sigma_g^2 \rightarrow 1\pi_g^2$ transition. This excitation should be doubly degenerate since excitations of two electrons can take place to the same π orbital giving rise to the $1^1\Delta_{g,x^2-y^2}$ diagonal double excitation or to different but degenerate π orbitals contributing to the $1^1\Delta_{g,xy}$ off-diagonal double. The $1^1\Delta_{g,xy}$ excitation (shown in Table I) does not couple to the vector \tilde{V} and the predictions of ERPA and ERPA2 (and also TD-APSG) are identical and amount to 4.20 eV, which is in agreement up to 0.09 eV with the CCSD value. The $1^1\Delta_{g,x^2-y^2}$ excitation energy predicted by ERPA2 equals 4.19 eV so it is almost perfectly degenerate with its off-diagonal counterpart. In case of ERPA the diagonal double $1^1\Delta_{g,x^2-y^2}$ excitation is missing. The RPA method,

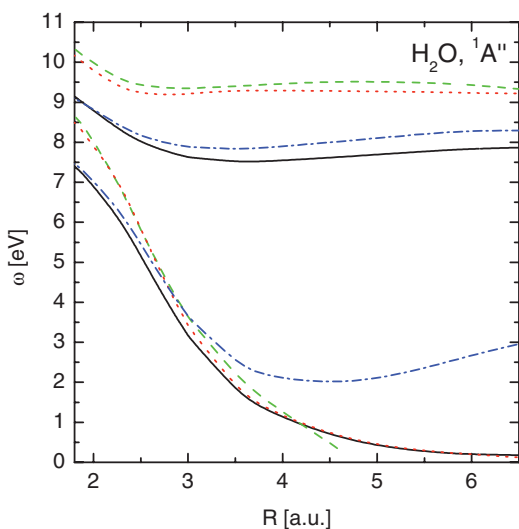


FIG. 5. Potential energy curves of the $1A''$ excited states for the H_2O molecule with one dissociating bond. Solid lines: CCSD, dotted lines: TD-APSG, dashed-dotted: TD-lrAPSG, and dashed lines: RPA results.

on the other hand, is unable to give predictions to pure double excitations so it misses both $1^1\Delta_{g,x^2-y^2}$ and $1^1\Delta_{g,xy}$ excitations.

The performance of the APSG methods is quite different for BH—another six-electron molecule. Fig. 2 and the pertinent data collected in Table I show that ERPA2 (since TD-APSG yields very similar results to ERPA2 we focus on the latter method) performs well for single excitations both around equilibrium geometry and when the bond is stretched. However, it fails badly in predicting double excitations. $1^1\Sigma^+$ excitation energies for a dissociating molecule require a contribution from the diagonal doubles, thus ERPA2 (and TD-APSG) outperforms the ERPA and RPA methods that miss such contributions. Around equilibrium geometry, the excitation to the third $1^1\Sigma^+$ state is of a double character. Since the second $1^1\Sigma^+$ excitation energy predicted by ERPA2 or TD-APSG does not bear any signature of a double character (no significant contribution from the \tilde{V} vector) it should be rather assigned to the $4^1\Sigma^+$ state as it has been done in Table I. One concludes that ERPA2 (and TD-APSG) misses the excitation to $3^1\Sigma^+$ state. This conclusion is confirmed by confronting Fig. 2, which clearly shows that around the equilibrium geometry the second ERPA2 curve follows the third $1^1\Sigma^+$ CCSD excitation, which is a single excitation. When the bond is stretched the ERPA2 smoothly switches to parallel the second $1^1\Sigma^+$ CCSD excitation. The latter acquires a single character for R exceeding 3.5 a.u. By looking at Fig. 2 one notices, however, that the RPA $3^1\Sigma^+$ excitation energies match quite closely the corresponding CCSD results around the equilibrium geometry. This agreement must be coincidental since RPA is unable to capture double excitation character (a double excitation character is indicated with dots in Fig. 2). As expected, RPA fails for the first two $1^1\Sigma^+$ excitations in the dissociation limit. Fig. 3 presents the potential energy curves corresponding to $1^1\Delta$ excitations that do not couple to the \tilde{V} vector. For such excitations ERPA, ERPA2, and TD-APSG methods yield identical results. Dots visible on curves in Fig. 3 indicate a double character of excitations predicted by the APSG or CCSD methods. The first ERPA curve follows the undotted CCSD curves methods around equilibrium geometry and in the stretched bond region so ERPA provides a correct description of the single $1^1\Delta$ excitation. As it can be seen in Table I and Fig. 3 the APSG methods do not miss a double $1^1\Delta$ excitation (it is identified as the lowest $1^1\Delta$ excitation with nonzero $\tilde{X}_{pq}, \tilde{Y}_{pq}$ elements with the p and q indices pertaining to $1\pi_x$ and $1\pi_y$ orbitals) but it is in a large error amounting to 2.72 eV with respect to the CCSD value at equilibrium geometry. It should be mentioned, however, that for the double $1^1\Delta$ excitation the CCSD model is not accurate either so we have included in Fig. 3 results obtained from the CC3 model that is reliable for the considered excitation.²³ The error of the CCSD method with respect to CC3 is still much smaller than a difference between the ERPA and CCSD results.

Since the ground state APSG method recovers less electron correlation with the number of electrons growing it is expected that for larger molecules the accuracy of single excitations around the equilibrium geometry predicted by the TD-APSG method (or ERPA2) will parallel that of

the RPA. For dissociating molecules TD-APSG (and ERPA2) should still outperform RPA in describing excitations that involve significant contributions from bonding and antibonding orbitals. For such excitations RPA fails as it has been already shown for diatomic molecules. The results compiled in Table II and Figs. 4 and 5 confirm these predictions. For water molecule at equilibrium geometry (cf. Table II) the TD-APSG excitations (ERPA2 values coincide with TD-APSG up to a few hundreds eV and they are not shown) are only slightly (by less than 0.15 eV if compared with the CCSD data) more accurate than those of RPA. The excitation energies predicted by TD-APSG are seriously overestimated and the absolute errors with respect to the CCSD results for the considered states range from 0.98 eV for 1^1B_2 to 1.16 eV obtained for 1^1B_1 state. Potential energy curves for the first $1^1A'$ and $1^1A''$ excitation energies presented in Figs. 4 and 5, respectively, are correctly described by the TD-APSG method for asymmetrically dissociating water molecule. A dominating contribution to the first $1^1A'$ excitation (in both CCSD and TD-APSG approximations) originates from an excitation from the orbital describing the OH_a bond of a constant length (composed of mainly the $2p_y(O)$ and $1s(H_a)$ atomic orbitals) to the antibonding orbital (its occupancy achieves a value 1/2 in the dissociation limit) related to a breaking bond composed of $2p_x(O)$ and $1s(H_b)$ orbitals. Similarly, the $1^1A''$ excitation is a single excitation from a $2p_z(O)$ orbital to the above mentioned antibonding orbital. The second $1^1A'$ excitation involves a bonding and antibonding pair of orbitals (their occupancies tend to 1/2 in the dissociation limit) describing OH_b bond breaking. Surprisingly, the TD-APSG curve corresponding to this excitation does not parallel its CCSD counterpart. Since TD-APSG is expected to work well for a bonding-antibonding excitation a deviation between the two methods may indicate that the CCSD method is not a good reference here. We have therefore computed the CC3 $1^1A'$ excitation energy curves of water and included the results in Fig. 4. The CC3 results confirm that the $2^1A'$ CCSD excitations are inaccurate for a stretched-bond molecule but the error of the TD-APSG method with respect to CC3 is still much larger. In case of the second $1^1A''$ excitation energy presented in Fig. 5 the TD-APSG curve parallels that of the RPA method rather than the CCSD curve. This behavior is understandable since the considered excitation does not include contributions from the orbitals involved in breaking the OH_b bond. Rather, it is localized on the OH_a group with the unstretched bond.

One may wonder if the performance of the TD-APSG method for single excitations at equilibrium geometry can be improved by adopting the approach presented in Sec. III based on the range-separation of the electron-electron interaction. To illustrate the performance of the TD-IrAPSG method and to point out its possible deficiencies we have applied it for water and formaldehyde molecules. Results compiled in Table II show that employing range-separation greatly reduces the error of the TD-APSG method. For H_2O the absolute errors decrease from around 1 eV to 0.05, 0.04, 0.30, and 0.35 eV for 1^1B_1 , 1^1A_2 , 2^1A_1 , and 1^1B_2 states, respectively. Unfortunately, it can be observed in Figs. 4 and 5 that improvement around the equilibrium geometry of the TD-APSG method provided by its range-separated version,

TD-IrAPSG, takes place at the cost of deteriorating a good performance of TD-APSG in the dissociating molecule. For the CH_2O molecule we first note that TD-APSG performs significantly better than RPA only for the first 1^1A_1 excitation for which the RPA and TD-APSG absolute errors with respect to the CCSD value amount to 0.60 and 0.16 eV, respectively. It is interesting to notice that the ERPA value for this excitation equals 10.50 eV so it is largely overestimated when compared with the TD-APSG or CCSD predictions. This observation indicates that even though the considered 1^1A_1 excitation is of a single character, including diagonal double elements as it is done in the TD-APSG (or ERPA2) approach leads to improving the results. The range-separated approach does not reduce the (already small) error for the 2^1A_1 state further but it lowers significantly the errors for the other considered states (cf. Table II). Namely, for the TD-IrAPSG approach the errors drop to 0.13, 0.31, and 0.15 eV for 1^1A_2 , 1^1B_2 , and 1^1B_1 excitations, respectively. A similar reduction of error has been observed by Rebolini *et al.* after applying the range-separation in the TD-HF method.¹⁷

VI. CONCLUSIONS

We have discussed formalisms based on the antisymmetrized product of strongly orthogonal geminal theory leading to obtaining excitation energies. The ERPA and ERPA2 methods, first proposed in Ref. 10, are derived from the equation of motion of Rowe, while TD-APSG [Eq. (33)], proposed in this paper, originates from the time-dependent linear response theory applied to the APSG wavefunction. The ERPA2 and TD-APSG approaches take into account the effects of diagonal double excitations [in case of ERPA2 diagonal doubles are explicitly included in the excitation operator given in Eq. (9)] that ERPA lacks completely. Consequently, ERPA2 and TD-APSG provide more accurate description of excitations coupling to diagonal doubles through nonzero elements of the vectors \tilde{V} and \tilde{W} [cf. Eqs. (18) and (33)] than ERPA. It has been shown that diagonal doubles are of particular importance in reproducing correctly fully symmetric $1^1\Sigma$ states of Li_2 and BH molecules in stretched-bond geometries, which is in line to what has been observed for H_2 in Ref. 14. Unfortunately, diagonal double contributions are insufficient to recover all double excitations. In case of the BH molecule the second $1^1\Sigma^+$ excitation, which is of a double character at equilibrium geometry, is missing in not only ERPA but also in ERPA2 and TD-APSG approaches. In case of excitations not coupling to diagonal doubles all three methods become identical. For such excitations there is no contribution from \tilde{V} or \tilde{W} vectors and therefore the only possibility to capture a double nature of some excitations arises due to a fact that the underlying APSG ground state wavefunction is multiconfigurational. This mechanism is apparently adequate to recover a correct value of the (off-diagonal) double $1^1\Delta_g$ excitation energy of Li_2 [cf. Table I]. On the other hand, the first $1^1\Delta$ double excitation of the BH molecule is in an error exceeding 2 eV (see Fig. 3) that indicates the need to include explicitly off-diagonal double excitations in the ERPA2 excitation operator. This would, however, increase drastically the computational cost of the method.

Although the origins of the EPRA2 and TD-ASPG approaches are different we have observed that both methods yield very similar results and the differences of excitation energies stay within a few hundreds eV for all considered molecules. We have already mentioned above that for excitations not coupling to diagonal doubles both methods provide identical excitation energies. But in Sec. III we have also shown that for the coupling excitations (including nonzero contributions from the $\tilde{\mathbf{V}}$ vector) the positive solutions to the ERPA2 equations are expected to be close to that of TD-APSG if excitations include mainly intrageminal contributions.

By noticing that the APSG functional, Eq. (2), is an example of the phase including natural orbital functional [cf. Eq. (7)] we have shown that the TD-APSG equations are identical to the time-dependent linear response PINO equations proposed by Giesbertz *et al.*⁶ This observation supports a claim given in Refs. 14 and 29 that the linear response of the natural occupation numbers, Eq. (42), is linked to predicting correctly some double excitations.

For larger molecules the performance of the APSG methods for single excitations around equilibrium geometry is expected to parallel that of the TD-HF. It has been already observed for the H₂O and CH₂O molecules. The superiority of the APSG-based methods is still apparent in describing excitations localized on breaking bonds, which is nicely illustrated in Figs. 4 and 5 for H₂O. Range-separation reduces the error of the TD-APSG around the equilibrium geometry as we have shown for water and formaldehyde in Table II but a correct performance of the TD-APSG for dissociating bonds is lost when a short-range LDA kernel is employed in calculations.

ACKNOWLEDGMENTS

This work was supported by the Foundation for Polish Science and the European Regional Development Fund under Grant No. POMOST/2010-1/6.

APPENDIX: DEFINITIONS OF THE RELEVANT APSG-BASED MATRICES

The matrices \mathbf{A}^+ , \mathbf{A}^- , \mathbf{D}^+ , and \mathbf{E}^+ present in the ERPA and ERPA2 equations, Eqs. (10) and (18), respectively, are given in terms of the elements of the \mathbf{A} and \mathbf{B} matrices that read

$$\begin{aligned} \forall_{\substack{p \neq q \\ r \neq s}} B_{pq,rs} &= A_{pq,rs} = -(n_q - n_p)(h_{qs}\delta_{rp} - h_{sp}\delta_{rq}) \\ &+ c_r(c_q\delta_{I_r I_q} + c_p\delta_{I_r I_p})(\langle sr|pq\rangle + \langle rs|pq\rangle) \\ &+ n_r[n_q(1 - \delta_{I_r I_q}) - n_p(1 - \delta_{I_r I_p})](\langle qr|sp\rangle - \langle qs|rp\rangle) \\ &- \delta_{rp} \sum_t (c_q\delta_{I_r I_q} + c_r\delta_{I_r I_r})c_t \langle tt|sq\rangle \\ &- \delta_{rq} \sum_t (c_p\delta_{I_r I_p} + c_r\delta_{I_r I_r})c_t \langle tt|ps\rangle \end{aligned}$$

$$\begin{aligned} &- \delta_{rp} \sum_t [n_q(1 - \delta_{I_r I_q}) - n_p(1 - \delta_{I_r I_p})]n_t \langle qt|st\rangle \\ &+ \delta_{rq} \sum_t [n_q(1 - \delta_{I_r I_q}) - n_p(1 - \delta_{I_r I_p})]n_t \langle st|pt\rangle, \end{aligned} \quad (\text{A1})$$

$$\begin{aligned} \forall_{p \neq q} B_{pq,rr} &= B_{rr,pq} \\ &= 2c_r(c_q\delta_{I_r I_q} + c_p\delta_{I_r I_p})\langle rr|pq\rangle \\ &- 2c_r(\delta_{rq} + \delta_{rp}) \sum_s c_s\delta_{I_r I_s} \langle ss|pq\rangle, \end{aligned} \quad (\text{A2})$$

$$\begin{aligned} \forall_{p,q} B_{pp,qq} &= 4c_p c_q \left\{ \delta_{I_q I_p} \langle qq|pp\rangle \right. \\ &\left. + \delta_{pq} \left[2 \sum_r n_r(1 - \delta_{I_q I_r}) \langle qr|qr\rangle + 2h_{qq} - \mu_{I_q} \right] \right\}. \end{aligned} \quad (\text{A3})$$

The integrals with a double bar are defined in Eq. (22) and $\{\mu_{I_p}\}$ are Lagrange multipliers obtained from stationary equations for the expansion coefficients $\{c_p\}$

$$\begin{aligned} \forall_p \mu_{I_p} c_p &= 2c_p h_{pp} + \sum_q c_q \delta_{I_q I_p} \langle qq|pp\rangle \\ &+ 2c_p \sum_q (1 - \delta_{I_p I_q}) n_q \langle pq|pq\rangle \end{aligned} \quad (\text{A4})$$

that result from taking derivatives with respect to the coefficients c_p from the sum of the APSG energy functional (2) and the normalization conditions $\mu_{I_p} (\sum_{q, I_q=I_p} c_q^2 - 1)$.

The TD-APSG equations given in Eq. (33) employ additionally the matrices \mathbf{D}^- and \mathbf{E}^- of the forms

$$\begin{aligned} \forall_{p > q} (c_p - c_q) D_{pq,r}^- &= 2c_r(\delta_{rp} - \delta_{rq})h_{qp} + (\delta_{rp} - \delta_{rq}) \sum_s c_s\delta_{I_r I_s} \langle ss|pq\rangle \\ &+ (c_p\delta_{I_r I_p} - c_q\delta_{I_r I_q})\langle rr|pq\rangle \\ &+ 2(\delta_{rp} - \delta_{rq})c_r \sum_s (1 - \delta_{I_r I_s})n_s \langle qs|ps\rangle \\ &+ 2c_r[n_p(1 - \delta_{I_r I_p}) - n_q(1 - \delta_{I_r I_q})]\langle qr|pr\rangle, \end{aligned} \quad (\text{A5})$$

$$\begin{aligned} \forall_{pq} E_{pq}^- &= \delta_{I_p I_q} \langle pp|qq\rangle \\ &+ \delta_{pq} \left[2 \sum_r n_r(1 - \delta_{I_q I_r}) \langle qr|qr\rangle + 2h_{qq} - \mu_{I_q} \right] \\ &+ 4c_p c_q (1 - \delta_{I_p I_q}) \langle pq|pq\rangle. \end{aligned} \quad (\text{A6})$$

Definitions of the matrices utilized in the time-dependent range-separated APSG equations, Eq. (46), read

$$\forall_{\substack{p > q \\ r > s}} (\mathbf{A}_\mu^+)_{pq,rs} = A_{pq,rs}^+ [\{h_{pq}^\mu\}, \{\langle pq|rs\rangle_\mu\}], \quad (\text{A7})$$

$$\forall_{\substack{p > q \\ r > s}} (\mathbf{A}_\mu^-)_{pq,rs} = A_{pq,rs}^- [\{h_{pq}^\mu\}, \{\langle pq|rs\rangle_\mu\}] + 4(c_p + c_q)(c_r + c_s)K_{pqrs}^{SR}, \quad (\text{A8})$$

$$\forall_{\substack{p > q \\ r}} (\mathbf{D}_\mu^+)_{pq,r} = D_{pq,r}^+ [\{h_{pq}^\mu\}, \{\langle pq|rs\rangle_\mu\}], \quad (\text{A9})$$

$$\forall_{\substack{p > q \\ r}} (\mathbf{D}_\mu^-)_{pq,r} = D_{pq,r}^- [\{h_{pq}^\mu\}, \{\langle pq|rs\rangle_\mu\}] + 4(c_p + c_q)c_r K_{pq,r}^{SR}, \quad (\text{A10})$$

$$\forall_{pq} (\mathbf{E}_\mu^+)_{pq,r} = E_{pq}^+ [\{h_{pq}^\mu\}, \{\langle pq|rs\rangle_\mu\}], \quad (\text{A11})$$

$$\forall_{pq} (\mathbf{E}_\mu^-)_{pq,r} = E_{pq}^- [\{h_{pq}^\mu\}, \{\langle pq|rs\rangle_\mu\}] + 8c_p c_q K_{ppq}^{SR}. \quad (\text{A12})$$

The short-range kernel, \mathbf{K}^{SR} , has been defined in Eq. (50). A convention has been adopted that the element $A_{pq,rs}^+ [\{h_{pq}^\mu\}, \{\langle pq|rs\rangle_\mu\}]$ is obtained by employing a definition for the matrix \mathbf{A}^+ given in Eqs. (14) and (A1) with the one-electron elements $\{h_{pq}\}$ replaced with $\{h_{pq}^\mu\}$ and the full-range two-electron integrals $\{\langle pq|rs\rangle\}$ replaced with their long-range counterparts $\langle pq|rs\rangle_\mu$ defined in Eq. (47).

¹P. R. Surján, *Topics in Current Chemistry* (Springer-Verlag, Berlin, 1999), Vol. 203, pp. 63–88.

²A. C. Hurley, J. Lennard-Jones, and J. A. Pople, *Proc. R. Soc. London* **A220**, 446 (1953).

³W. Kutzelnigg, *J. Chem. Phys.* **40**, 3640 (1964).

⁴V. A. Rassolov, *J. Chem. Phys.* **117**, 5978 (2002).

⁵P. R. Surján, A. Szabados, P. Jeszenszki, and T. Zoboki, *J. Math. Chem.* **50**, 534 (2012).

⁶K. J. H. Giesbertz, O. V. Gritsenko, and E. J. Baerends, *Phys. Rev. Lett.* **105**, 013002 (2010).

⁷K. J. H. Giesbertz, O. V. Gritsenko, and E. J. Baerends, *J. Chem. Phys.* **133**, 174119 (2010).

⁸P. R. Surján, *Croat. Chem. Acta* **71**, 489 (1998).

⁹Y. U. Dmitriev and G. Peinel, *Int. J. Quantum Chem.* **19**, 763 (1981).

¹⁰K. Chatterjee and K. Pernal, *J. Chem. Phys.* **137**, 204109 (2012).

¹¹T. Arai, *J. Chem. Phys.* **33**, 95 (1960).

¹²R. van Meer, O. V. Gritsenko, K. J. H. Giesbertz, and E. J. Baerends, *J. Chem. Phys.* **138**, 094114 (2013).

¹³D. J. Rowe, *Rev. Mod. Phys.* **40**, 153 (1968).

¹⁴K. J. H. Giesbertz, K. Pernal, O. V. Gritsenko, and E. J. Baerends, *J. Chem. Phys.* **130**, 114104 (2009).

¹⁵A. Savin in *Recent Developments and Applications of Modern Density Functional Theory*, edited by J. M. Seminario (Elsevier, Amsterdam, 1996), pp. 327–357.

¹⁶E. Fromager, S. Knecht, and H. J. A. Jensen, *J. Chem. Phys.* **138**, 084101 (2013).

¹⁷E. Rebolini, A. Savin, and J. Toulouse, *Mol. Phys.* **111**, 1219 (2013).

¹⁸K. Pernal, *J. Chem. Phys.* **136**, 184105 (2012).

¹⁹O. Gritsenko, K. Pernal, and E. J. Baerends, *J. Chem. Phys.* **122**, 204102 (2005).

²⁰S. Piazani, S. Moroni, P. Gori-Giorgi, and G. B. Bachelet, *Phys. Rev. B* **73**, 155111 (2006).

²¹T. H. Dunning, *J. Chem. Phys.* **90**, 1007 (1989).

²²A. Schäfer, C. Huber, and R. Ahlrichs, *J. Chem. Phys.* **100**, 5829 (1994).

²³H. Koch, O. Christiansen, P. Jørgensen, and J. Olsen, *Chem. Phys. Lett.* **244**, 75 (1995).

²⁴O. Christiansen, H. Koch, P. Jørgensen, and J. Olsen, *Chem. Phys. Lett.* **256**, 185 (1996).

²⁵M. Schreiber, M. R. Silva-Junior, S. P. Sauer, and W. Thiel, *J. Chem. Phys.* **128**, 134110 (2008).

²⁶DALTON, a molecular electronic structure program, Release 2.0, 2005, see <http://www.kjemi.uio.no/software/dalton/dalton.html>.

²⁷O. Christiansen, H. Koch, and P. Jørgensen, *J. Chem. Phys.* **103**, 7429 (1995).

²⁸K. J. H. Giesbertz, O. V. Gritsenko, and E. J. Baerends, *J. Chem. Phys.* **136**, 094104 (2012).

²⁹K. J. H. Giesbertz, E. J. Baerends, and O. V. Gritsenko, *Phys. Rev. Lett.* **101**, 033004 (2008).